We are IntechOpen,
the world's leading publisher of
Open Access books
Built by scientists, for scientists

6,900
Open access books available

186,000
International authors and editors

200M
Downloads

154
Countries delivered to

Our authors are among the

TOP 1%
most cited scientists

12.2%
Contributors from top 500 universities

CLARIVATE ANALYTICS
BOOK
CITATION
INDEX
INDEXED

WEB OF SCIENCE™

Selection of our books indexed in the Book Citation Index
in Web of Science™ Core Collection (BKCI)

Interested in publishing with us?
Contact book.department@intechopen.com

Consolidation of AISI316L Austenitic Steel — TiB2 Composites by SPS and HP-HT Technology

Iwona Sulima

Additional information is available at the end of the chapter

1. Introduction

Quickly developing industry and need for materials of better utility parameters contribute to development of innovative production technologies. Industry is always in search of new technologies which meet growing demands of faster better and cheaper products. Powder metallurgy is modern technology of manufacturing of ceramic, metallic and composite products. Commonly applied technologies of the powder metallurgy based on the sintering process include following stages:

i.   Obtaining of the powders; the aim is obtaining of adequate chemical and phase composition of a powder of certain physical and technological properties. The powders are attained among others through: processing of natural raw materials, chemical synthesis, size reduction, segregation and other methods.

ii.   Product formation; a process due to which powder is prepared giving it respective shape through pressing, drawing, casting from a slurry. During the pressing process itself, the following phenomena occur:

- particles of the powder come close at a distance allowing adhesion,
- increase of contact surface area of the powder due to relocation and their plastic deformation,
- peeling the oxide coating off through abrasion of the neighbouring particles,
- and local point sintering of the particles due to plastic deformation and increase of temperature.

iii.   Sintering; main operation of the technology of the powder metallurgy, which is conducted until diffusion connection of the powder particles is established.

iv.   Processing of the sinters; the final stage after which the product is ready to use.

The sintering process itself is a process depending on transforming of the powder material into new stable material with different physical properties. The characteristic feature of the technology is possibility of serial production of ready elements and semi-products of the highest quality and strictly specified composition, without impurities and faults connected with conventional technological procedures of plastic processing or foundry. Besides, parsimony in the use of materials, energy, time and automation of the process make the method very economical and prospective. Therefore, in recent years, the interest in modern sintering methods in the production processes has increased [1-4].

Sintering is the process involving many quantitative and qualitative factors. The first group of the factors affecting the sintering are values characterizing a preformed product from a power, such as: particle size of the powder, its chemical and phase composition, density of a profile, inhomogeneity of the profile. On the other hand, the second group of the factors make parameters controlled during the sintering process such as: temperature, time, pressure, sintering atmosphere. It is also to remember about so called random factors, which, in uncontrolled way, may influence the result of sintering, e.g. inhomogeneous chemical composition or inhomogeneity of mixtures [1].

From the mentioned above three groups of factors influencing properties and microstructure of the sintered materials, the most important are the following:

• Temperature of sintering, which should ensure successful finalizing consolidation processes and receiving of required utility properties. It should be selected in such a way, that during consolidation, diffusion mechanisms causing solidifying contraction dominated.

• Time of sintering is the time during which the sintering material is kept at the sintering temperature. Carefully chosen time allows for effective course of diffusion mechanisms in a material and limits also the process of grains growth.

• Pressure; application of the external load causes intensification of the consolidation processes and, among others, simplifies the elimination process of pores at the final stages of the sintering. Due to application of pressure, temperature can be lowered and time of sintering can be shorter.

• Atmosphere of sintering; during the sintering process, neutral (protective) or active atmosphere can be applied. In most cases the process is realized in the neutral atmosphere, whose main advantage is protection of the sintering materials again oxidation. This kind of atmospheres are selected in such a way, so possible reaction with a sinter is forbidden. On the other hand, the active atmospheres directly influence the sintering process causing desirable changes of the chemical composition, *eg.* prevent decomposition of the compound before finish of the sintering or reduce oxides present in the powder that impede sintering etc.

• Activators of sintering are used in order to accelerate contraction, decrease sintering temperature or formation of proper microstructure of a sinter. They influence mainly

acceleration of diffusion processes, formation of transient liquid phase and prevent grain growth [1,4-8].

Among techniques limiting grain growth and accelerating consolidation are sintering under pressure (Hot Isostatic Pressing (HIP) and High Pressure – High Temperature (HP-HT) or microwave sintering or the one taking advantage of current impulses. The main advantage of the sintering by HP-HT method is opportunity to achieve extremely high pressures together with high temperatures during the process. It is worth noting, that under influence of simultaneous operation of pressure and temperature, the process proceeds much faster (usually time does not exceed few minutes) than in the case of free sintering (which usually lasts from few to several hours). The obtained sinters are characterized by a degree of densification reaching almost 100% and isotropic properties. The use of such conditions can also reduce the diffusion of particles and prevent grain growth. The high-pressure devices are composed of hydraulic presses and specially-designed chambers that permit sintering. Presently, many solutions for such high-pressure chambers exist. Basic types of the chambers applied in industry are the following: spherical chambers of Bridgman type, 'Belt' type chambers and multi-die cubic chambers. Such construction solutions of the synthesis chamber allow for relatively large volume of reaction charge, optimal distribution of pressure and achievement of high sintering temperature. Their characteristic feature is attaining quasi-hydrostatic state of stress through stable medium transferring pressure, such as various kinds of rocks, most often. The highest possible temperature at which the sintering process can be carried by means of HP-HT method is 2000°C, or even more – depending on the duration of the sintering process [9-11]. The HP-HT method is applied to sintering large group of materials, for example: diamond [10], cubic boron nitride (cBN) [12], TiB_2 ceramics [13], gradient materials [14,15], composite materials [12,16-19] and others.

In recent years, many papers were published on new techniques of sintering, in which heating of charge is performed by impulse current source. Taylor is recognized as a progenitor of this technology [20], who in 1933 proposed a pioneering solution involving to heat up during sintering Joule heat released during current flow through the consolidating powder. This process was named resistance sintering (RS). Currently, large interest in this kind of sintering is connected with its technical and economical advantages. The resistance sintering allows to obtain dense sinters with good properties at lower temperature and short time (from few to several minutes) [21]. The RS techniques involving pulsed current include Pulse Plasma Sintering (PPS) and Spark Plasma Sintering (SPS) methods. The SPS method was developed in 1960 initially to sinter metal powders [22]. However, due to high cost of equipment and low efficiency of the sintering process, the solution has not found its application at the beginning. Only in 80's of the 20th century, a new generation of apparatus for sintering of materials was elaborated under a name Spark Plasma Sintering. The SPS method was used even then to produce modern composite and functional gradient materials [23,24]. Up till now, not all phenomena associated with pulsed current sintering have been explained. There are many theories regarding the SPS sintering. Yoshimura *et al.* proved experimentally [25] that consolidation intensifies processes caused by the pulsed current.
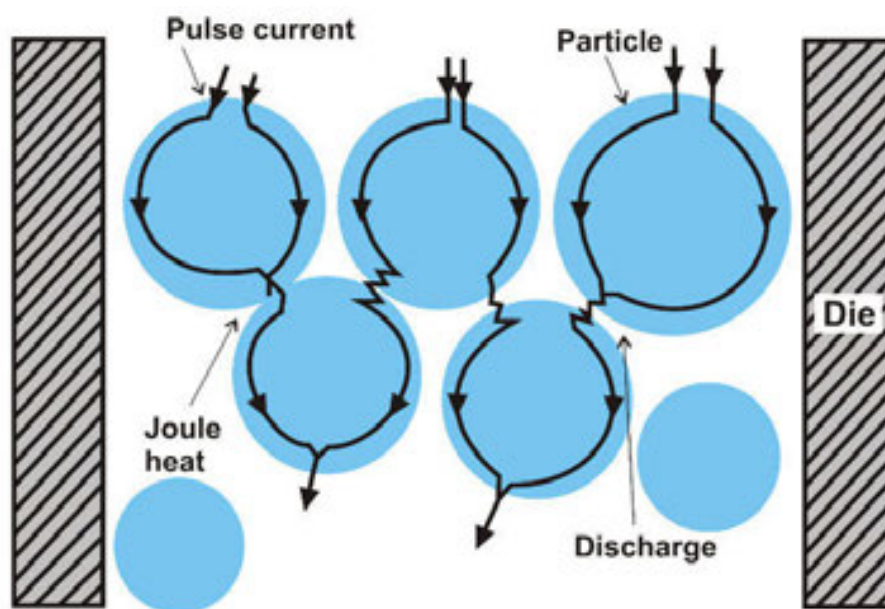
Figure 1. A schematic drawing of the pulsed current that flows through powder particles [26]

Currently accepted concept basis on the phenomenon of electric discharge. Heating up of the sintered materials is caused by pulsed current that may flow in two ways: either through graphite die and punches or through press powder particles. At the moment of current flow through powder particles, electric discharge occurs at places, where particles touch each other and at free spaces in the material (Figure 1). As a result, in these regions, a momentary increase of temperature even up to several dozen thousands degrees of Celsius is observed. The heat in the process concentrates at surface of the particles. Then, vaporizing occurs followed by cleaning, activation of the sample surface and increase of diffusion processes on the surface and grain boundaries. Next, partial melting takes place and formation of necks between particles being connected [27-29]. The pulsed current during SPS sintering is usually applied during consolidation of materials that conduct electric current. On the other hand, insulators must be consolidated with the application of the direct current. Main advantages of the SPS method are as follows:

- shortening of the time of sintering, what prohibits the grain grow of materials,

- enabling fast densification under relatively low temperatures,

- elimination of application of the sintering agents in the case of many materials,

- faster and better purifying and activation of the powder particle surfaces, what enhances sintering activity,

- consolidation of materials without the application of the initial pressing, isostatic densification and drying [26,29,30].

Thanks to SPS method, sinters of the following materials were produced in the recent years: metals and their alloys (eg. Fe, Cu, Al, Au, Ag, Ni, Cr, Ti, Mo etc.), oxide ceramics (eg. Al_2O_3,

MgO, ZrO_2, TiO_2, SiO_2), carbides (eg. SiC, B_4C, TiC, ZrC, WC), nitrides (eg. TiN. Si_2N4, TaN, ZrN, AlN), borides (eg. TiB_2, ZrB_2, HfB_2, VB_2), fluorides (eg. LiF, CaF_2), composite materials and intermetallic phases [24, 25, 31-35].

Currently, the TiB_2 compound belongs to the group of modern engineering ceramics. The interest in this material has been developing since the beginning of 2000. Previously, the use of TiB_2 was limited for technological reasons. TiB_2 ceramics is characterised by a unique combination of physico-chemical properties that allow it to be used under the conditions of high temperature and in corrosive environments. The most attractive properties of TiB_2 are:

• high hardness (33 GPa),

• high tensile strength (350 MPa),

• high compression strength 4900 MPa,

• the bending strength of 305-521MPa obtained for products sintered in the temperature range of 1600-1900°C,

• high Young's modulus (570 GPa) stable with increasing temperature,

• high melting point (3127°C),

• low density (4.5-4.62 g/cm^2).

Titanium diboride is also characterised by a very good resistance to oxidation, chemical and structural stability at high temperatures, thermal shock resistance and abrasion resistance [36-38]. Currently, TiB_2 ceramics is an attractive material for specific applications in the aviation, automotive, defence, and aerospace industries, including the production of armours for land vehicles, ships and planes, aerospace parts and parts operating at high temperatures, characterised by very good abrasion resistance. Restrictions on more extensive use of TiB_2 ceramics are mainly due to difficulties associated with the sintering process and obtaining in this way a pure ceramic material of suitable density. They include, among others:

• a very high melting point,

• low coefficient of diffusion along the grain boundaries, requiring a long time of sintering,

• presence of oxide layers of TiO_2 and B_2O_3 adversely affecting the compaction process and reaction with metal matrix [39,40].

Despite these difficulties of purely technological character, recent years have brought an increased interest in titanium diboride, with focus on its use as a phase reinforcing the metal matrix composites. Technical literature [41-46] presents studies that relate to the use of TiB_2 ceramics as a reinforcing phase of composites based on, among others, iron, aluminium, copper, titanium, or cobalt, and on their respective alloys. Authors of the research works focus their attention mainly on studies of the effect of the amount of the reinforcing phase on the properties and microstructure of these composites and on the development of best technology for their manufacture. In the composites reinforced with particles of TiB_2, an important issue is to choose the right size of the reinforcing phase and at the same time its optimum percent

content in the composite material. Depending on the volume fraction and particle size of each material, sintered products with highly varied microstructure and properties can be obtained. Studies described in [48,49] show the impact of TiB_2 ceramics on microstructure and tribological as well as mechanical properties of austenitic stainless steel sintered by HIP. Nahme et al. [47] studied the mechanical properties of AISI 316L stainless steel reinforced with 15 vol% of TiB_2, including its behaviour at elevated temperatures. An improvement was obtained in the Young's modulus (218 GPa), tensile strength (885 MPa) and compression strength (1800 MPa) of the sintered materials. As proved by various research works, the deformation of sintered AISI 316L stainless steel reinforced with 15 vol% of TiB_2 was significantly reduced from 45% to 6%. Microstructural observations revealed a uniform distribution of TiB_2 ceramics in the examined material and presence of phases rich in Cr/Mo in places where the grains of this ceramics appeared. Tjong et al. [48] examined the properties of AISI 304 austenitic stainless steel reinforced with varying amounts of TiB_2 ceramics. It has been shown that increasing the content of the reinforcing TiB_2 phase improved both hardness and tensile strength, but at the expense of reduced ductility. Based on the tribological tests carried out, a dramatic improvement of abrasion resistance has been obtained with increased volume fraction of the ceramic phase.

The aim of the presented study was to analysis of the effect of sintering techniques on the physical, mechanical and tribological properties of 316L austenitic steel-TiB_2 composites.

2. Materials and research methodology

2.1. Materials selected for sintering composites

The TiB_2 powder (2.5-3.5μm in average size, 99.9 wt.% in purity) and commercial AISI 316L austenitic stainless steel (25μm in average size, Hoganas) were used in the present study. The stainless-steel powder have the chemical composition as follows: 17.20 wt.% Cr, 12.32 wt.% Ni, 2.02 wt.% Mo, 0.43 wt.% Mn, 0.89 wt.% Si, 0.03 wt.% S, 0.028 wt.% P, 0.03 wt.% C and balance of Fe. Figure 2 presents the morphology of the selected powders.

The raw powders were mixed in the special, closed container using the mixer of TURBULA type. The powders were mixed for 8 hours. The initial phase composition of mixtures for the samples preparation were as follow:

- Steel AISI 316L+2 vol% TiB_2

- Steel AISI 316L+4 vol% TiB_2

- Steel AISI 316L+6 vol% TiB_2

- Steel AISI 316L+8 vol% TiB_2

For composition analysis, the AISI 316L austenitic stainless steel was used.
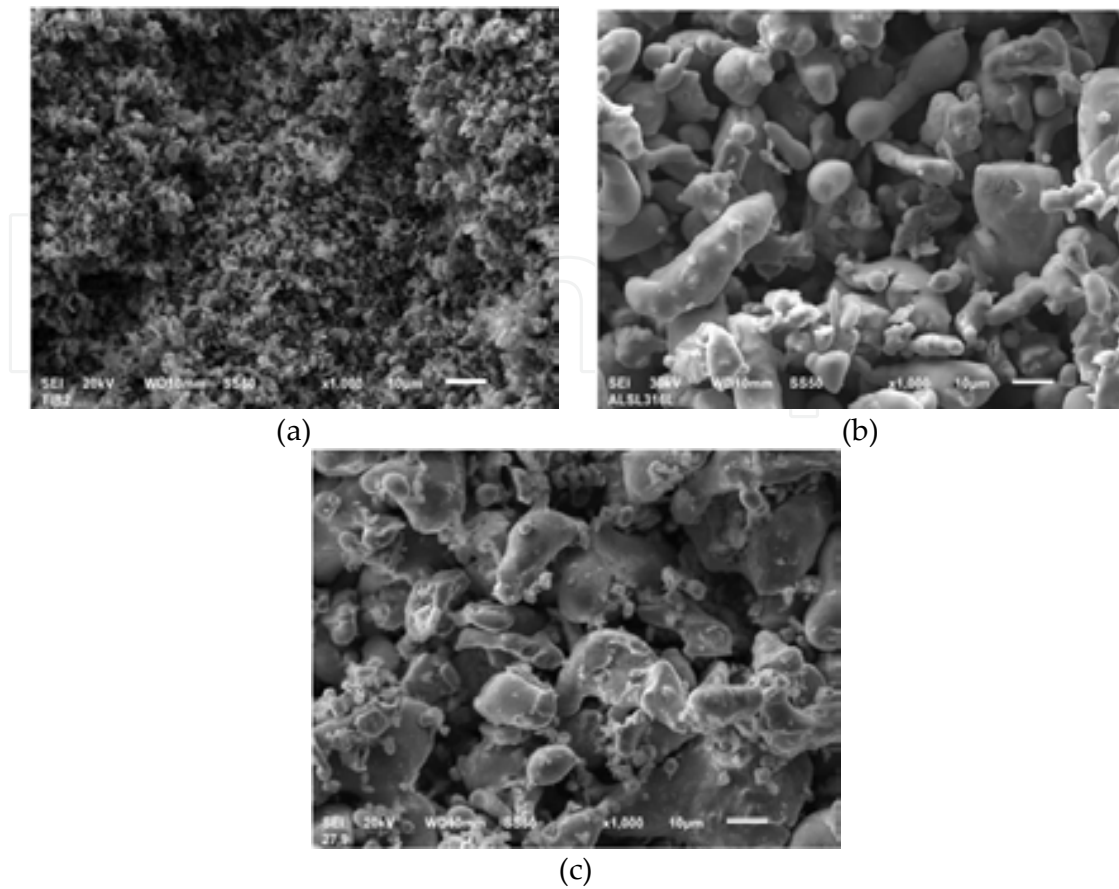
(a)   (b)

(c)

Figure 2. Morphology of powders of: a) titanium diboride, b) AISI 316L austenitic stainless steel and c) mixtures of steel with 8 vol% TiB$_2$ used in current study.

2.2. Fabrication of composites

Consolidation of composites reinforced with various volume fractions of TiB$_2$ were performed by High Pressure-High Temperature (HP-HT) and Spark Plasma Sintering (SPS). First, for the densification of composites the high pressure–high temperature (HP–HT) Bridgman type apparatus was used. Figure 3 presents the scheme of Bridgman-type HP-HT apparatus. The samples were sintered at temperature of 1000°C and 1300°C pressure of 5 ± 0.2 GPa for 60 seconds. In the case this methods, the samples had a size: 15 mm in diameter, 5 mm in high.

Next, the SPS process was carried out using the HPD 5 FCT System GmbH furnace. Materials are compacted in a graphite die using a maximum pressure of 35 MPa at vacuum. Maximum pressure was obtained after duration of 10 minutes. Vacuum and pressing time of 10 minutes was to vent the mixture. After that, the SPS furnace chamber introduced argon, which acted as a protective gas and the sintering process was carried out. The heating rate and holding time were 200°C*min^{-1} and 30 minutes, respectively. In the case this methods, the samples had a size: 20 mm in diameter, 7 mm in high. Figure 4 shows the schematic of Spark Plasma Sintering (SPS).
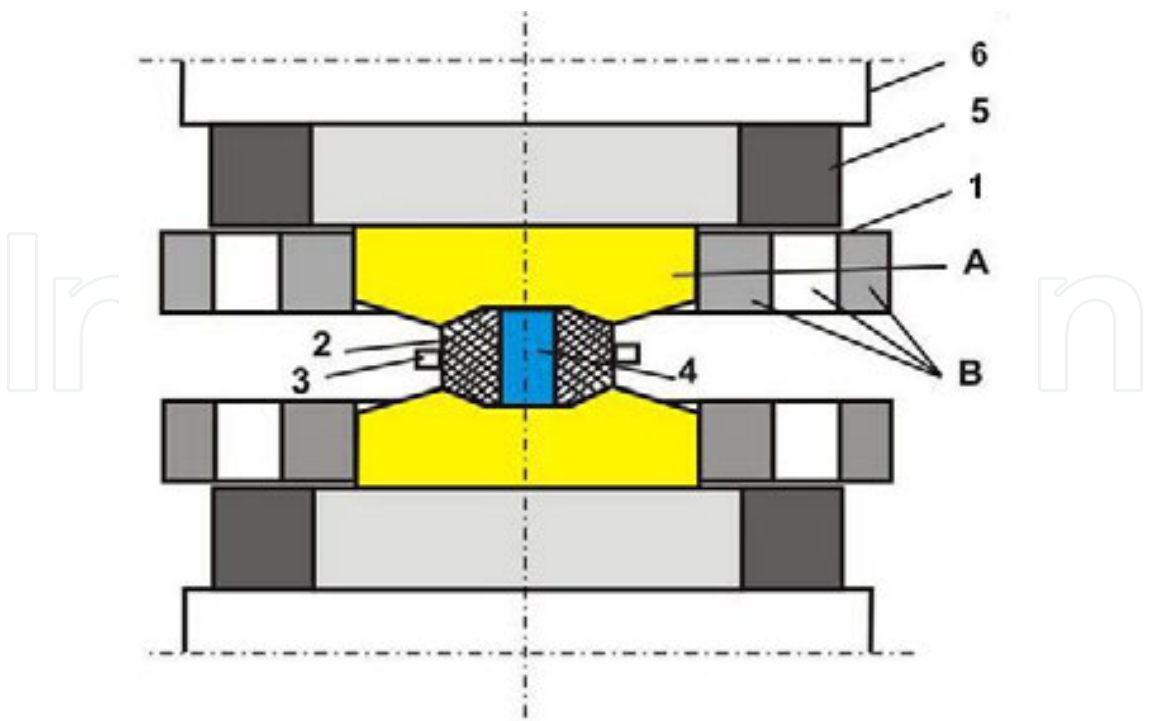
Figure 3. Scheme of Bridgman-type, toroidal HP-HT apparatus: 1 – anvil (A – central part made of sintered carbides, B – supporting steel rings), 2– pyrophyllite container, 3 – pyrophyllite gasket, 4 – material for sintering, 5 – punch, 6 – supporting plate [11].
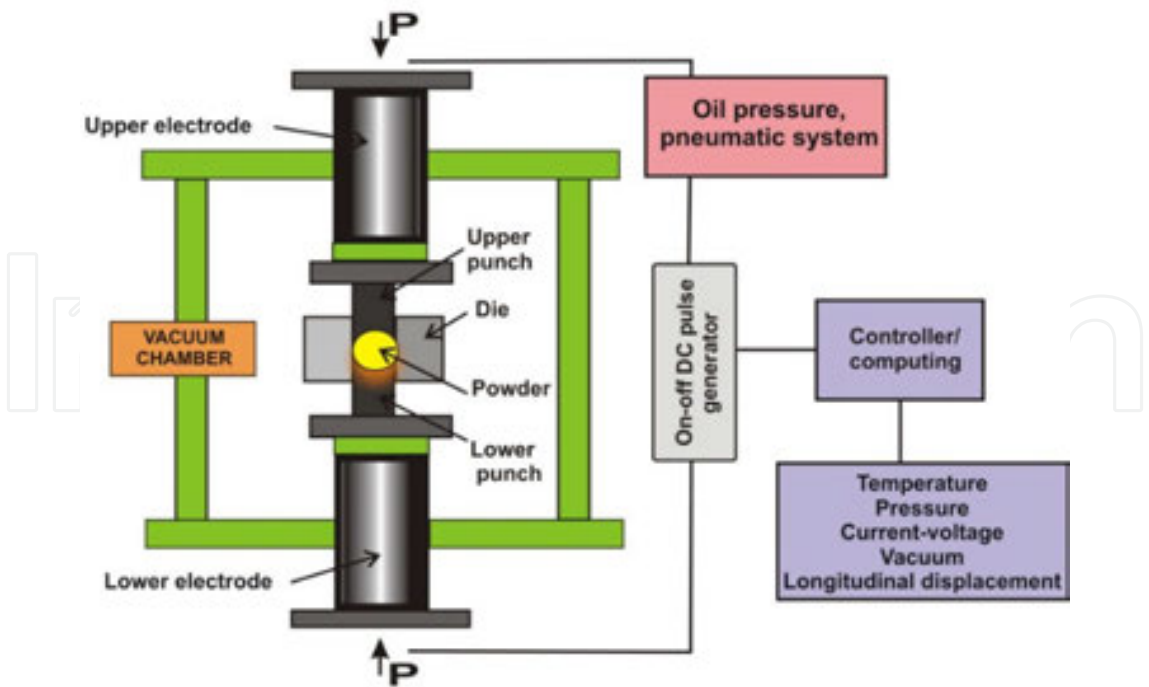

Figure 4. Spark plasma sintering device scheme.

2.3. Testing methods

Density was determined by weighing in air and water using Archimedes method. Uncertainty of measurements was 0.02 g/cm^3. Young's modulus of the composites were measured basing on the velocity of the ultrasonic waves transition through the sample using ultrasonic flaw detector Panametrics Epoch III. The velocities of transverse and longitudinal waves were determined as a ratio of sample thickness and relevant transition time. The accuracy of calculated Young's modulus is estimated at 2 %. Calculations were made using the following formula:

$$E = \rho C_T^2 \frac{3C_L^2 - 4C_T^2}{C_L^2 - C_T^2}$$

where: E-Young's modulus, C_L – velocity of the longitudinal wave, CT-velocity of the transversal wave, ρ-density of the material.

A JEOL JSM 6610LV scanning electron microscope with Energy Dispersive Spectrometry (EDS) and Hitachi SU-70 scanning electron microscope with Wavelength Dispersive Spectroscopy (WDS) were used for microscopy studies of composites. Also, the phase compositions of selected samples were analysed by X-ray diffraction (XRD) using Cu K radiation with a scintillation detector (Empyrean; PANalytical).

The Vickers microhardness (HV0.3) of the composite samples was measured at FM-7 micro-hardness tester. The applied load for non-graded materials was 2.94 N. Standard deviations of HV 0.3 values were no more than 4 % of the average values. The compression test was carried out at INSTRON TT-DM machine at strain rate of about of 10^{-3} s.

Tribological tests were performed using a ball-on-disc wear machine UMT-2T (producer CETR, USA). The experimental procedure followed the ISO 20808:2004(E) [49,50]. For ball-on-disk method the sliding contact is brought by pushing a ball on a rotating disc specimen under a constant load. The loading mechanism applies a controlled load F_n to the ball holder. The friction force was measured continuously during the test using the extensometer. For each test a new ball is used. Specimens were washed in high purity acetone and dried. After the ball and sample were mounted, materials are washed in ethyl alcohol and then dried. The wear test conditions were:

• ball made of Al_2O_3, diameter of 3.175 mm,

• friction track diameter: 4 mm,

• sliding speed: 0.1 m/s,

• total sliding distance: 200 m,

• test duration: 2000s,

• load applied: 4 N,

• room temperature.

The values of friction coefficient were calculated from the following equation:

$$\mu = \frac{F_f}{F_n L}$$

where F_f is the measured friction force, and F_n is the applied normal force, L – sliding distance [m].

Following the wear test, the specific wear rate was calculated. For the wear track on the disc specimen, the cross-sectional profile of the wear track at four places at intervals of 90° using a contact stylus profilometer was measured with accuracy of measurement in the vertical axis of 0.01 μm, in the horizontal axis of 0.1 μm. The cross-sectional area of the wear track was calculated using a custom-developed software. Specific wear rate according to wear volume was calculated by means of equation:

$$W_{V(disc)} = \frac{V_{disc}}{F_n L}$$

where: $W_{V(disc)}$ – specific wear rate of disc [mm³/Nm]; V_{disc} – wear volume of disc specimen [mm³]; F_n – applied load [N]; L-sliding distance [m].

The wear volume of disc specimen was calculated from following Equation:

$$V_{disc} = \frac{\pi}{2} R(S_1 + S_2 + S_3 + S_4)$$

where: R –radius of wear track [mm]; S_1 to S_4 – cross-sectional areas at four places on the wear track circle [m²].

The cross-sectional microstructure of worn surface was observed using a scanning electron microscope (SEM) JEOL JSM 6610LV.

3. Results

Figure 5 shows the results of measurements of the apparent density of the composite materials sintered by HP-HT and SPS. From these results (Figure 5a) it follows that all the materials sintered by HP-HT have reached a very high level of density, despite the short sintering time (60 sec). This was due to the combined effect of high pressure and high temperature during the HP-HT sintering process. The use of such sintering conditions allows restricting the diffusion and prevents growth of grains in the sintered materials. For composites sintered at 1300°C, the apparent density (Table 1) was in the range of 99-100% of the theoretical density. The apparent density was found to be decreasing with the increasing amount of the reinforcing TiB$_2$ phase in the composite matrix. This was the result of a much lower density of titanium diboride (4.52 g/cm² [55]) compared with the density of AISI 316L austenitic stainless steel (8.00

g/cm^2 [56]). The resulting sintered composites had low porosity. The porosity of the composites with various content of the TiB_2 ceramics was in the range of 0.004-0.017% (Table 1).
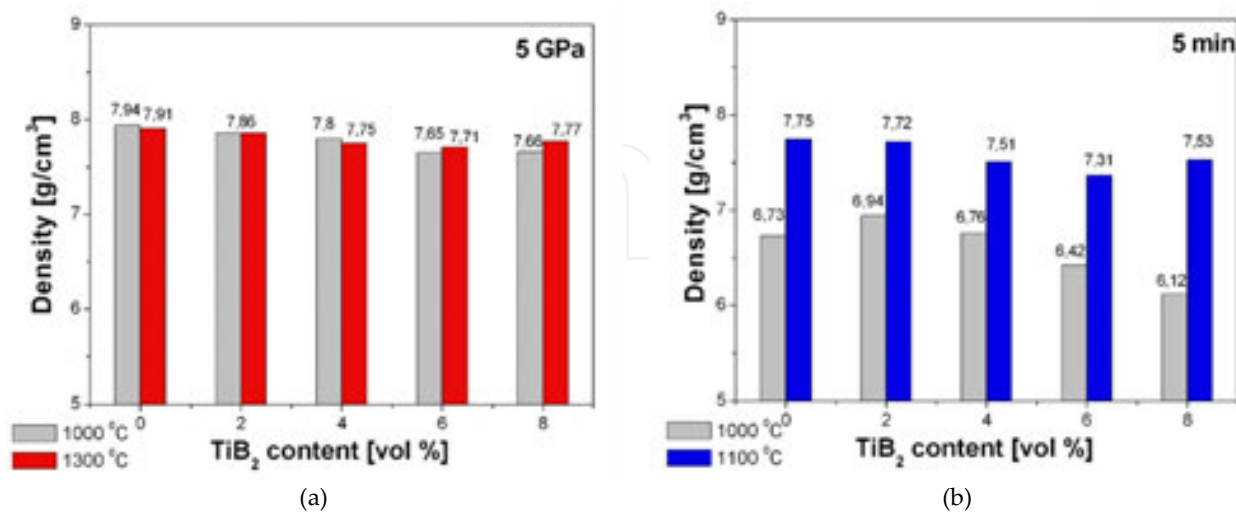

(c)

Figure 5. Effect of TiB_2 particle content and sintering methods: a) HP-HT [51,52] and b) SPS [53] on relative density of composites.

In contrast, analysing the results (Figure 5.b) of the apparent density measurements for the composites sintered by SPS, a strong correlation was noticed between the apparent density of the tested materials and the sintering temperature (Table 2). The apparent density was significantly improved with the increase of sintering temperature. The best density in the range of 97-99% of the theoretical density was obtained for the sintering temperature of 1100°C, while sinters produced at a temperature lower than 1000°C had the density of 82-88%. The temperature of 1000°C was not sufficient to obtain the required degree of consolidation in the austenitic steel-based composites reinforced with TiB_2 ceramics. Careful examination of the results has showed that the process of composite consolidation was most intense during the first few minutes of the SPS, producing the required degree of density (Figure 5b). Materials manufactured at 1000°C were characterised by high porosity in the range of 10.5-18.5% (Table 2). Increasing the sintering temperature to 1100°C has improved this parameter, and composite porosity was found to be at a level of 0.03-2.3%.

Sintered materials	Sintering conditions (HP-HT)		Relative density $\varrho0$ [g/cm^3]	$\frac{\varrho_0}{\varrho_{teor}}$ [%]	Porosity [%]	([-]	Young's modulus E [GPa]	$\frac{E}{E_{teor}}$ [%]
	T [°C]	p [GPa]						
steel AISI 316L	1000	5	7.94	100	0.005	0.30	190	91
	1300		7.91	100	0.004	0.31	192	94
steel AISI 316L+ 2vol% TiB_2	1000	5	7.86	100	0.006	0.30	197	91

Sintered materials	Sintering conditions (HP-HT)		Relative density $\varrho0$ [g/cm³]	$\frac{\varrho_0}{\varrho_{teor}}$ [%]	Porosity [%]	([-]	Young's modulus E [GPa]	$\frac{E}{E_{teor}}$ [%]
	T [°C]	p [GPa]						
	1300		7.86	100	0.004	0.30	205	94
steel AISI 316L+ 4vol% TiB$_2$	1000	5	7.8	100	0.005	0.30	202	90
	1300		7.75	99	0.010	0.29	209	93
steel AISI 316L+ 6vol% TiB$_2$	1000	5	7.65	99	0.009	0.29	208	91
	1300		7.71	99	0.011	0.29	215	94
steel AISI 316L+ 8vol% TiB$_2$	1000	5	7.66	100	0.007	0.29	207	88
	1300		7.77	100	0.004	0.29	216	93

Table 1. The selected physical properties of composites with the various content of TiB$_2$ sintered by HP-HT method [51,52].

Sintered materials	Sintering conditions (SPS)		Relative density $\varrho0$ [g/cm³] [54]	$\frac{\varrho_0}{\varrho_{teor}}$ [%]	Porosity [%]	([-]	Young's modulus E [GPa]	$\frac{E}{E_{teor}}$ [%]
	T [°C]	time [min]						
AISI 316L	1000	5	6.73	83	12.32	0.26	165	79
	1100		7.75	97	1.12	0.27	196	94
steel AISI316L+ 2vol% TiB$_2$	1000	5	6.94	88	10.55	0.29	138	64
	1100		7.72	98	0.03	0.27	207	96
steel AISI316L+ 4vol% TiB$_2$	1000	5	6.76	86	10.89	0.29	130	58
	1100		7.51	96	0.08	0.28	202	90
steel AISI316L+ 6vol%. TiB$_2$	1000	5	6.42	83	16.29	0.26	112	49
	1100		7.49	96	2.10	0.28	203	89
steel AISI316L+ 8vol% TiB$_2$	1000	5	6.29	82	18.27	0.27	166	67
	1100		7.53	98	0.034	0.28	215	91

Table 2. The selected physical properties of composites with the various content of TiB$_2$ sintered by SPS method.

Figure 6a shows the results of studies of the Young's modulus of materials sintered by HP-HT. The results demonstrate an obvious improvement in this parameter when the content of the reinforcing TiB$_2$ phase is increasing in the composite matrix. The highest values of Young's

modulus were obtained in the composites reinforced with 8 vol% of TiB_2 (Figure 6a). For comparison, Young's modulus was changing with the increasing content of the reinforcing phase from 197 GPa to 207 GPa for the sintering temperature of 1000°C, and from 192 GPa to 216 GPa for the sintering temperature of 1300°C, thus proving that the temperature of sintering also exerts an effect on this parameter (Table 1 and Figure 6a). With the application of temperature raised to 1300°C, higher values of the Young's modulus were obtained. Also in composites sintered by SPS, the temperature of sintering had a significant effect on the Young's modulus (Figure 6b and Table 2). At 1000°C, low values of the Young's modulus and a large scatter in the results of measurements (in the range of 112-176 GPa) were obtained. This might be due to the high porosity of materials sintered under such conditions. Raising the temperature to 1100°C considerably improved the values of Young's modulus (202-215 GPa). In general, it has been found that the temperature of 1000°C is not preferred in the case of the SPS method, since it does not ensure the required high physical properties of the tested materials.
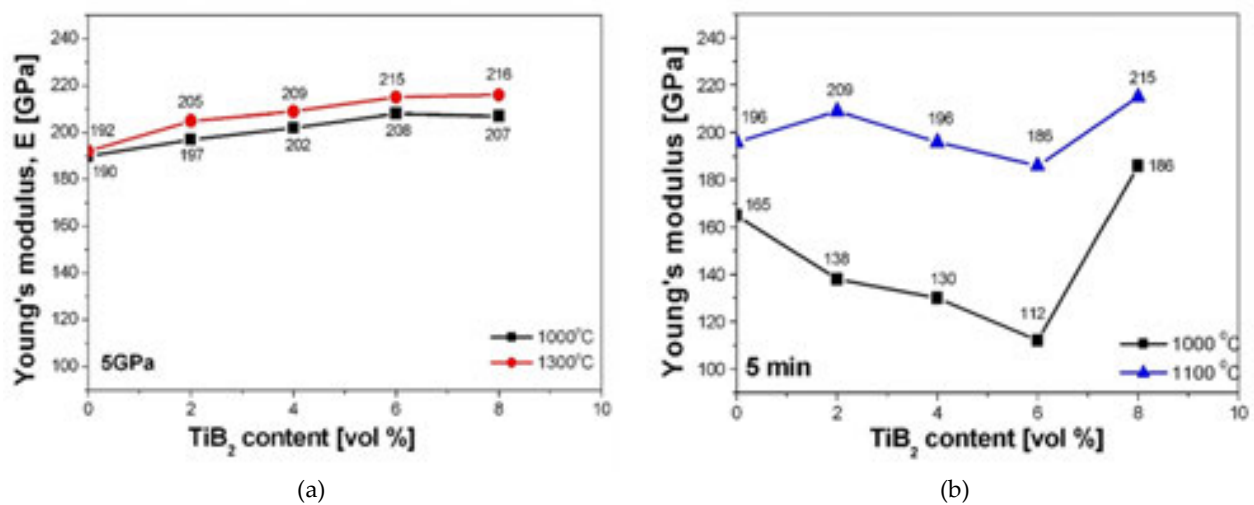

(a)   (b)

(c)

Figure 6. Effect of TiB_2 particle content in matrix and sintering methods: a) HP-HT [51,52] and b) SPS on Young's modulus of composites.

Figures 7 and 8 show examples of the microstructure produced in AISI 316L austenitic stainless steel and in the examined composites made by HP-HT and SPS. In all the composite materials, microstructural observations revealed a homogeneous distribution of the reinforcing TiB_2 phase in the composite matrix. The best effect of the uniform distribution of TiB_2 was obtained in the composites containing 6 vol% and 8 vol% of this compound (Figure 7de, 8de). In all the tested composites, the reinforcing TiB_2 phase had the tendency to settle along the matrix grain boundaries.

Microscopic observations have proved that composites obtained by the HP-HT technique were nearly free from porosity (Figure 7b-e). It was the result of a very high degree of consolidation during the sintering process and a very high level of the obtained density. Figure 7a shows the microstructure of AISI 316L austenitic stainless steel after sintering by HP-HT. A characteristic feature of this microstructure is the presence of fine and irregu-

lar austenitic grains of a few μm. A similar structure of the steel matrix was also observed in the composites with 2 vol% of TiB$_2$ (Figure 7b). On the other hand, the steel matrix in the composites with higher volume fraction of TiB$_2$ was characterised by a different type of morphology including oval-shaped grains with smooth boundaries. Microstructural analysis made by EDS and WDS (Figure 10,11) and X-ray studies (Figure 9a) confirmed the presence of titanium diboride in the form of dark precipitates settled at grain boundaries. All the investigated microstructures were observed to show the local presence of precipitates containing large amounts of nickel (Figure 11).

(a)

(b)

(c)

(d)

(e)
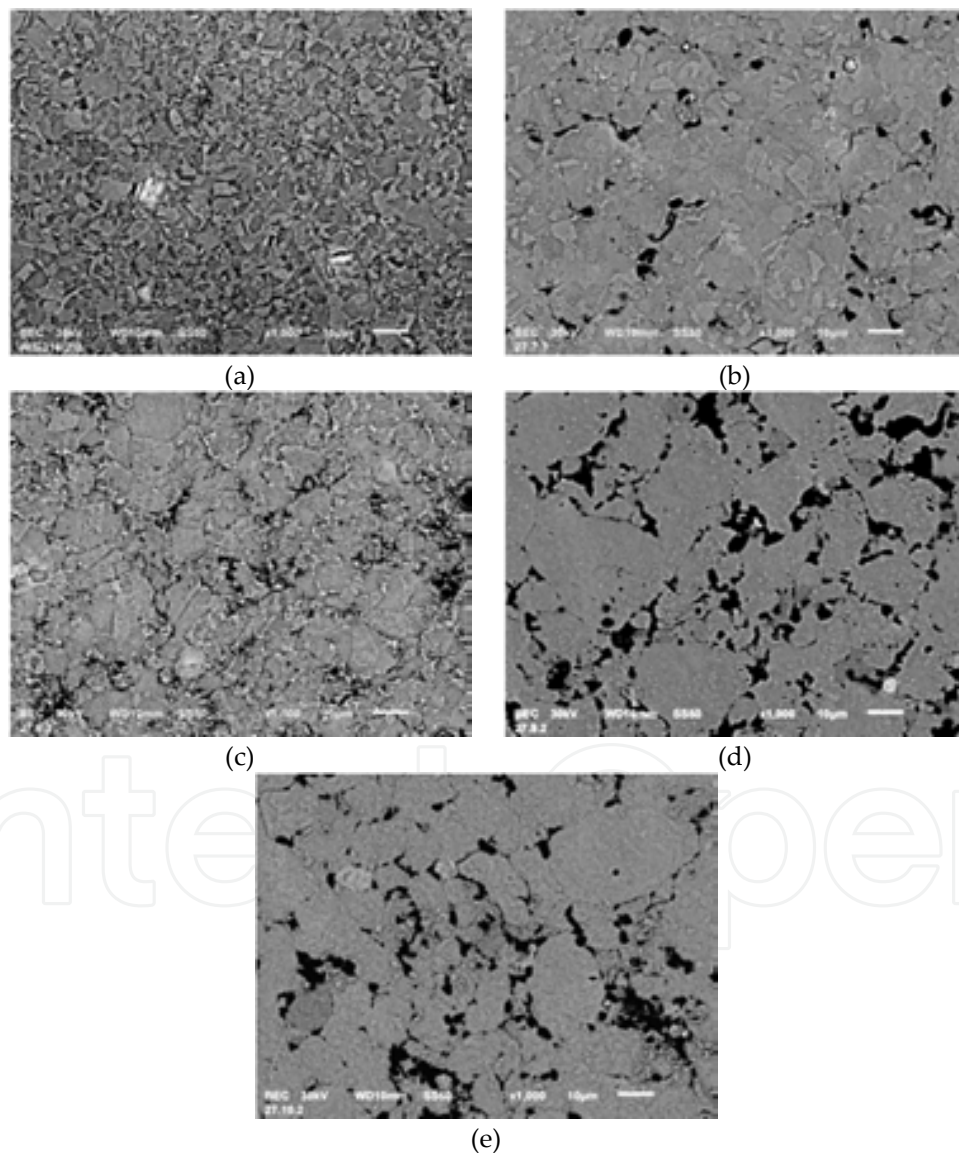
Figure 7. Selected micrographs: a) AISI 316L austenitic stainless steel and composite with: b) 2 vol.% of TiB$_2$ c) 4 vol% of TiB$_2$ d) 6 vol% of TiB$_2$ and e) 8 vol% of TiB$_2$ (HP-HT method, sintered at 1300°C and 5 GPa).

(a)

(b)

(c)

(d)

(e)
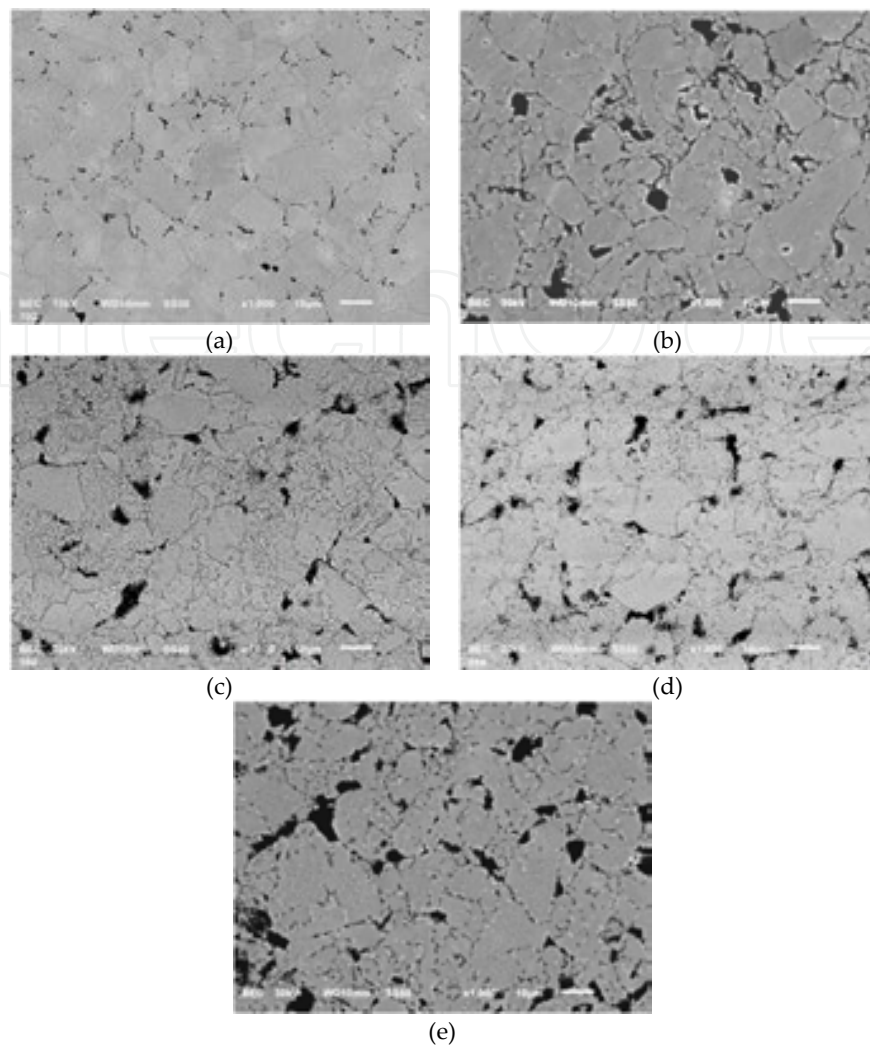
Figure 8. Selected micrographs: a) AISI 316L austenitic stainless steel and composite with: b) 2 vol% of TiB$_2$ c) 4 vol% of TiB$_2$ d) 6 vol% of TiB$_2$ and e) 8 vol% of TiB$_2$ (SPS method, sintered at 1100°C and 5 min).
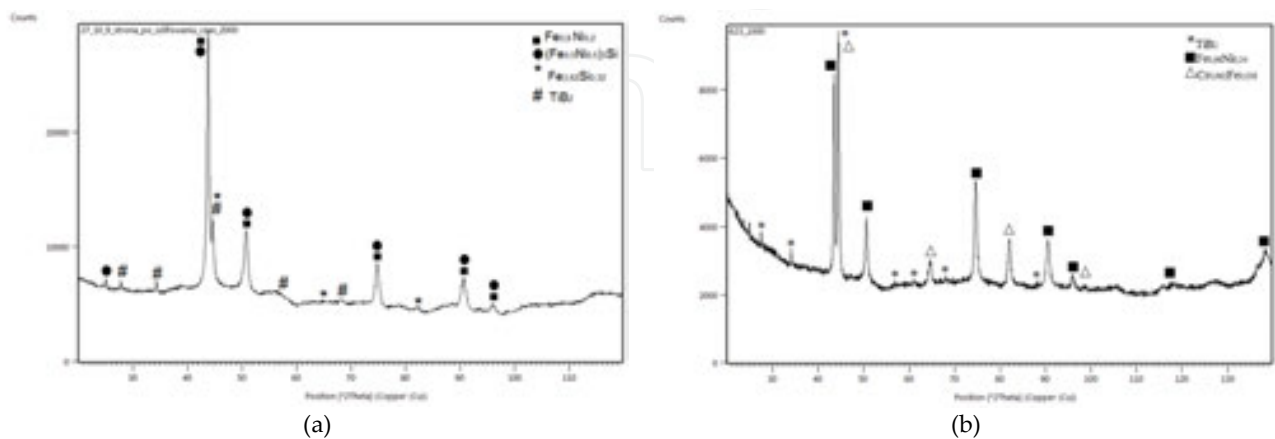

(a)

(b)

(c)

(d)

Figure 9. XRD patterns of the composites with 8 vol% TiB$_2$ particles obtained by HP-HT (1300°C) and SPS method (1100°C).

(e)

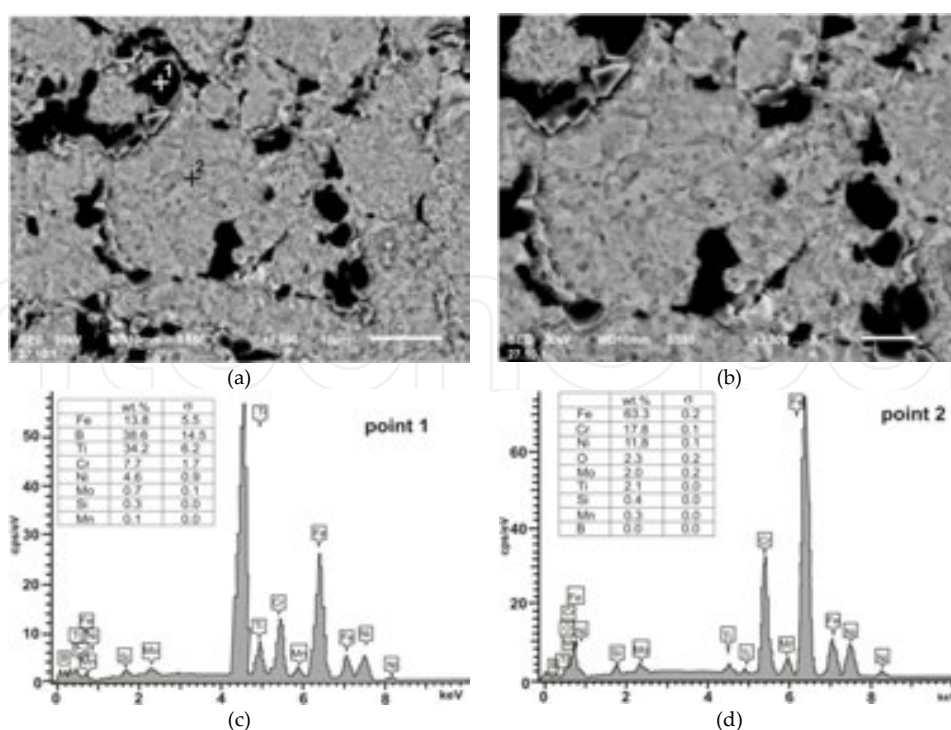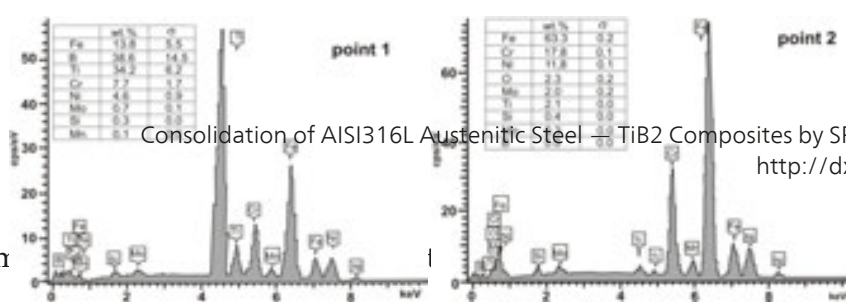**Figure 10.** (a, b) The microstructure of composites with 8 vol% of TiB_2 (HP-HT method, sintered at 1300°C, 5 GPa) and (c, d) corresponding point analysis (EDS).

In all the composites made by SPS, the microstructure of the steel matrix has prevailed, i.e. the one characterised by the presence of particles with regular oval shapes, along which the reinforcing TiB_2 phase was distributed (Figure 8b-d). Sinters obtained at a temperature of 1000°C showed some voids at the grain boundaries. In contrast, the composites sintered at 1100°C were nearly completely free from porosity. This demonstrates fully effective optimisation of the SPS sintering process and selection of the best sintering conditions. Differences were revealed in the microstructure of materials sintered by SPS as compared to the materials sintered by high-pressure method. Chemical analysis (EDS and WDS) of composites sintered by SPS disclosed in the microstructure the presence of numerous precipitates containing mainly chromium (Figure 12,13), while X-ray analysis (Figure 9b) further confirmed the presence of titanium diboride and chromium-containing phases. Additionally, in the immediate vicinity of TiB_2 ceramics (Figure 13, the formation of large precipitates with characteristic band substructure was observed (Figure 13). The examined results of microstructural studies clearly show that both the sintering method and the sintering conditions have a significant impact on changes in the microstructure of the tested composites. Application of the SPS method promotes the formation of new phases. Some attention deserves the fact that the SPS sintering process uses pulsed current for heating of the sintered materials. At the time of current flow through the grains, spark discharges take place at the grain contact points and in the void areas of the sinter. As a result of these effects, a temporary temperature increase (up to several thousand degrees Celsius) can be expected in the near-surface layer of particles. It is followed by evaporation, cleaning and activation of the sample surface and by the increased rate of diffusion on the surface and along the grain boundaries [29,30]. A combination of these

mechanism ... d brings changes to the microstructure of the tested composites.

Fig.10 (a, b) The microstructure of composites with 8 vol% of TiB₂ (HP-HT method, sintered at 1300°C, 5 GPa) and (c, d) corresponding point analysis (EDS).
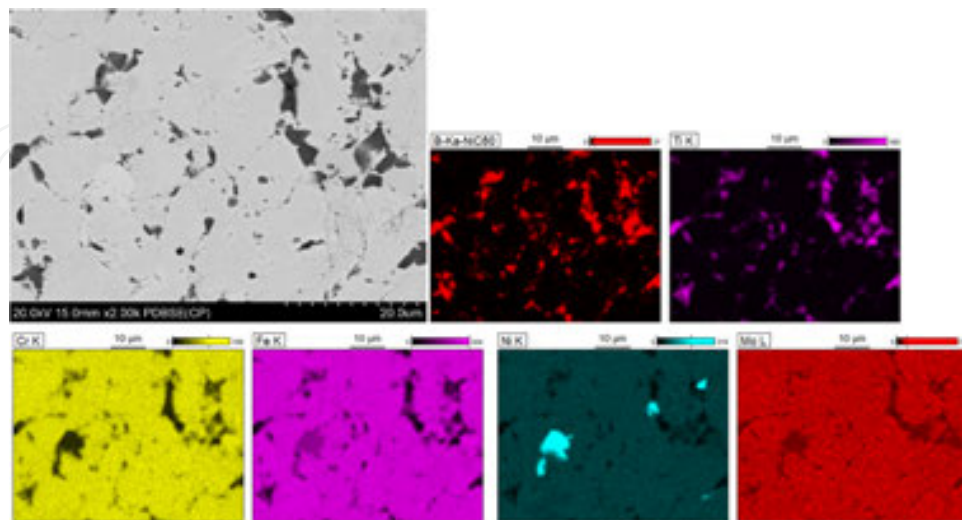

Fig. 11 The microstructure of composites with 8 vol% of TiB₂ (HP-HT method, sintered at 1300°C, 5 GPa) with corresponding area analysis (WDS)

Figure 11. The microstructure of composites with 8 vol% of TiB₂ (HP-HT method, sintered at 1300°C, 5 GPa) with cor-responding area analysis (WDS).

(a)   (b)

(c)   (d)
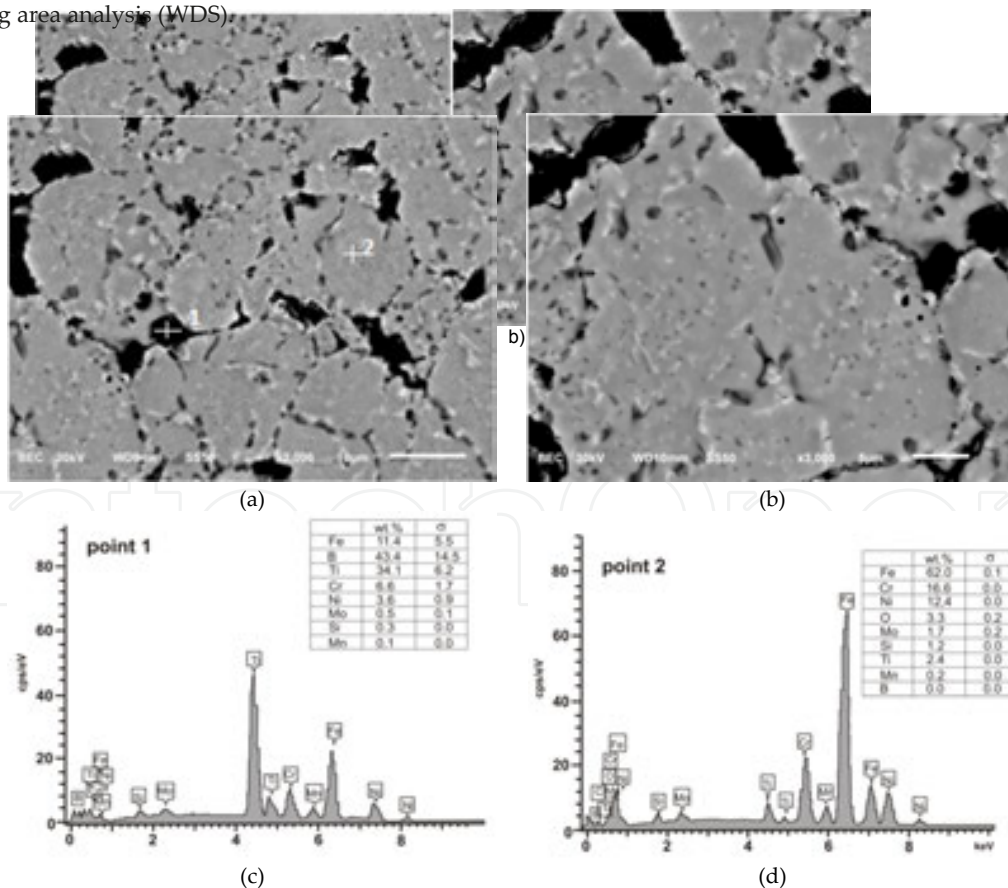
(e)

Figure 12. (a, b) The microstructure of composites with 8 vol% of TiB₂ (SPS method, sintered at 1100°C, 5 min) and (c, d) corresponding point analysis (EDS).
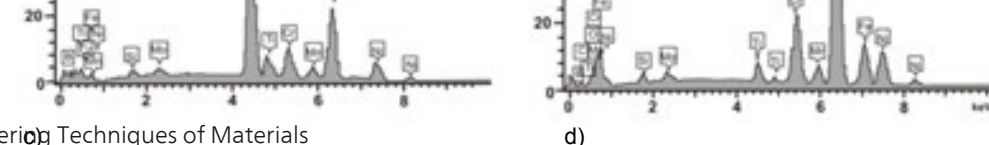
Fig.12 (a, b) The microstructure of composites with 8 vol% of TiB$_2$ (SPS method, sintered at 1100°C, 5 min) and (c, d) corresponding point analysis (EDS).
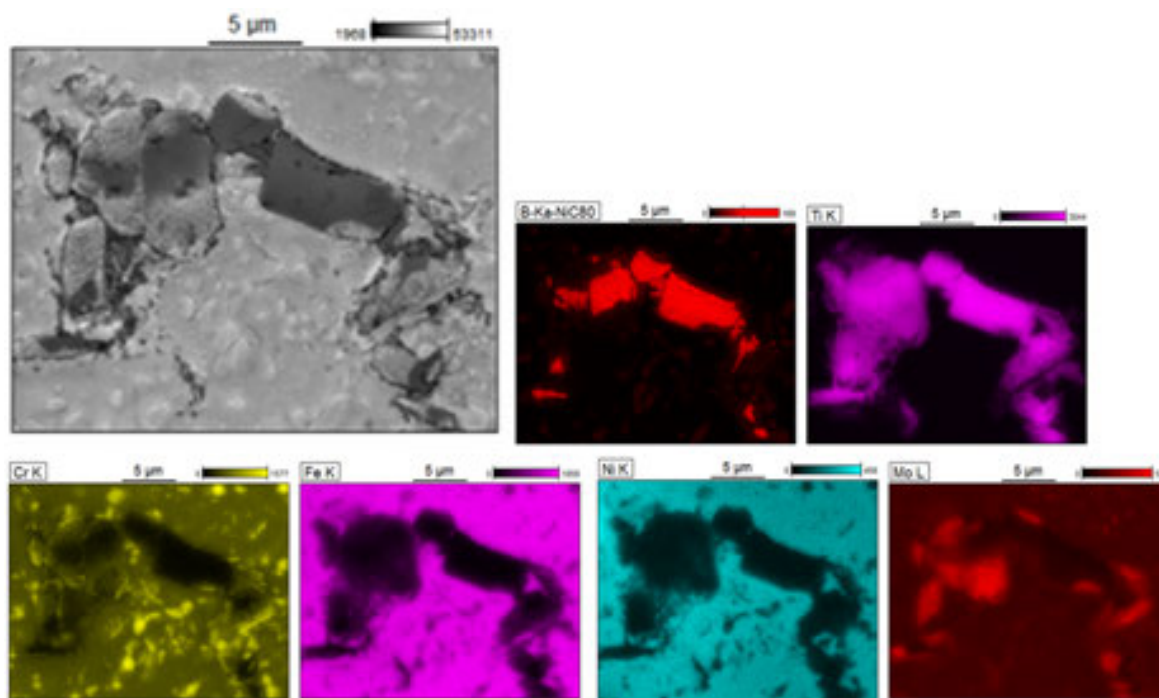

Figure 13. The microstructure of composites with 8 vol% of TiB$_2$ (SPS method, sintered at 1100°C, 5 min) with corresponding area analysis (WDS).

Figure 14 shows the results of microhardness measurements. In the case of the HP-HT method (Fig.14a), microhardness was found to be essentially dependent on the sintering temperature. In materials sintered at 1000°C, the microhardness higher by about 20-40%, compared to the microhardness of the composites sintered to be at 1300°C, was obtained. For example, in the composite with 8vol% of TiB$_2$, the microhardness was 368 HV0.3 and 282 HV0.3 for the temperature of 1000°C and 1300°C, respectively. All the composites sintered by SPS (Figure 14b) suffered a definite decrease of microhardness. For materials sintered at 1000°C and 1100°C, a very low level of microhardness was obtained. It was comprised in the range of 170-265 HV0.3 and depended on the TiB$_2$ content and sintering temperature.

The results of compression tests are shown in Figures 15-17. Careful analysis of the data obtained for composites sintered by HP-HT proves that the introduction of TiB$_2$ ceramics to the steel matrix significantly improves the mechanical properties of the tested composite materials (Figure 16), compared with the steel without reinforcement (Figure 15a). High content of the TiB$_2$ reinforcement in the composite matrix improves also the compression strength of this material. The compression strength of the steel without reinforcement was at a level of 580-730 MPa, depending on the sintering temperature (Figure 15a), while even the addition of TiB$_2$ as small as 2 vol% introduced to the steel matrix raised the strength to 1000-1160 MPa (Figure 16a). For composites with 8 vol% of TiB$_2$, the compression strength in the range of 1200-1300 MPa was obtained (Figure 16d). The compression curves of the composites sintered at a temperature lower than 1000°C (HP-HT method) were characterised by a large range of elastic deformation and more narrow range of plastic deformation. In contrast, in the composites obtained at 1300°C, the analysis of compression curves revealed a
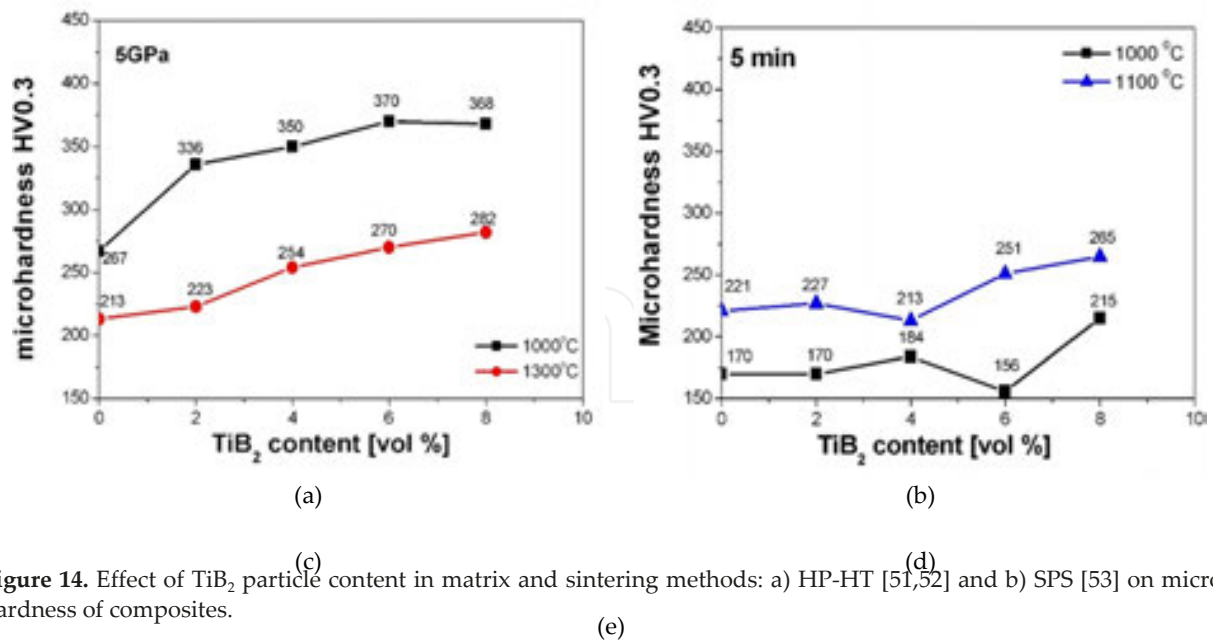
(a)   (b)

(c)

(d)

Figure 14. Effect of TiB$_2$ particle content in matrix and sintering methods: a) HP-HT [51,52] and b) SPS [53] on micro-hardness of composites.

(e)

large range of plastic deformation accompanied by a double reduction in the range of elastic deformation. All the composites sintered by SPS showed very similar characteristics of the stress-strain curve with a large range of plastic deformation (Figure 17). In general, the mechanical properties of composites sintered by SPS were inferior to the properties of composites sintered by high-pressure technique. The compression strength of the AISI 316L austenitic stainless steel without reinforcement was in the range of 520-780 MPa, depending on the sintering temperature (Figure15b). Composites sintered at 1100°C offered higher compression strength comprised in the range of 930-1040 MPa, depending on the content of the reinforcing phase in matrix (Figure 17).
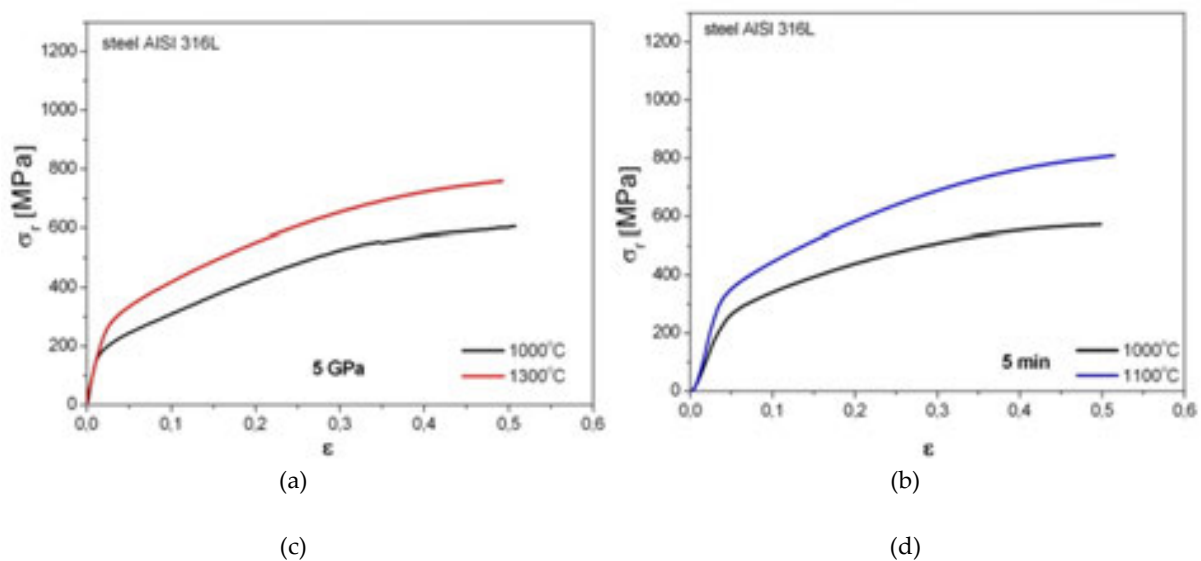

(a)   (b)

(c)   (d)

Figure 15. Compression strength of AISI 316L austenitic stainless steel sintered by: a) HP-HT and b) SPS methods.
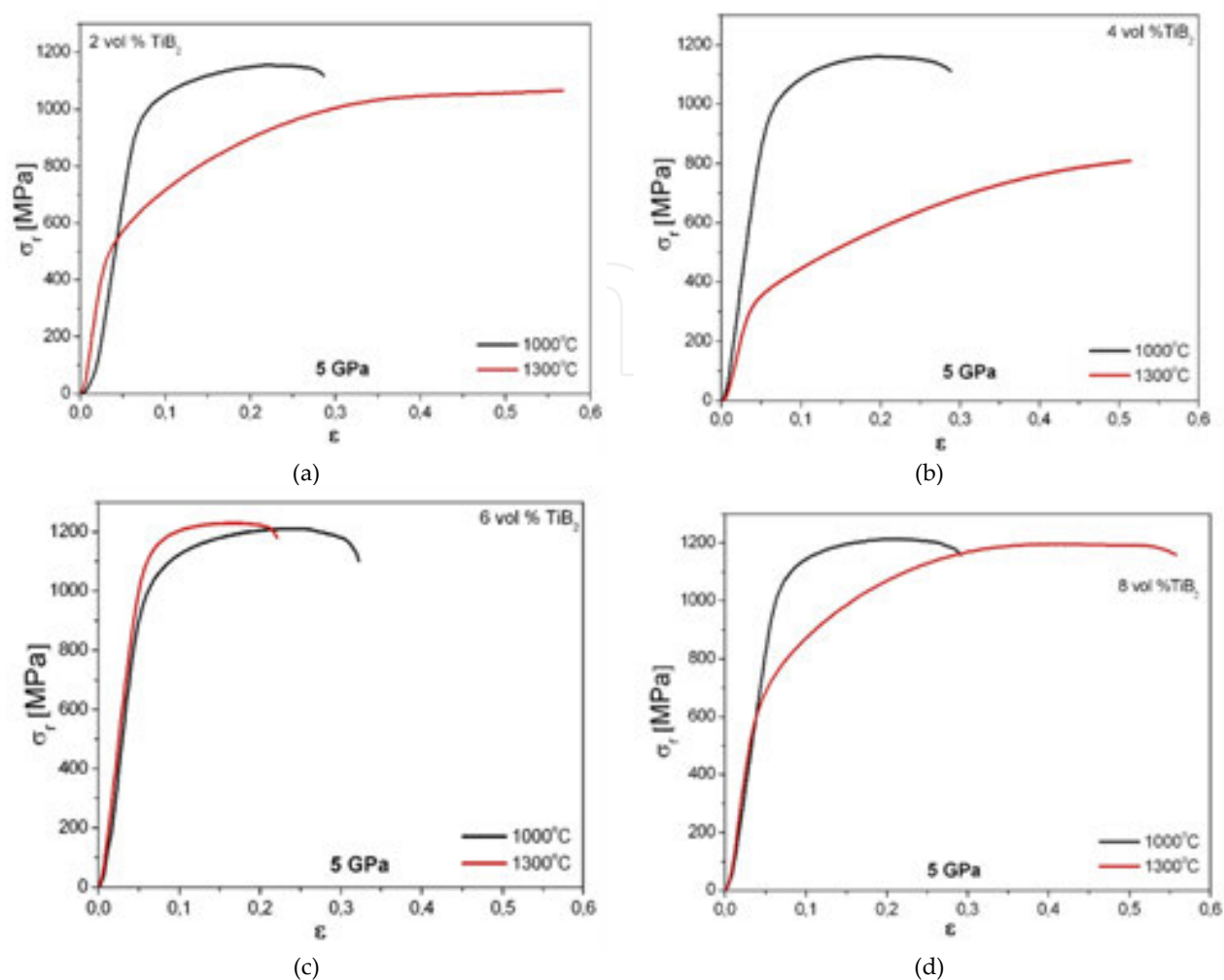
(e)

Figure 16. Compression strength of the composites with: a) 2 vol.% of TiB$_2$ b) 4 vol.% of TiB$_2$ c) 6 vol.% of TiB$_2$ and d) 8 vol.% of TiB$_2$ sintered by HP-HT method.

The results of studies of the coefficient of friction (μ) and the specific wear rate ($W_{v(disc)}$) are shown in Figures 18 and 19, respectively. Coefficient of friction depends on the content of TiB$_2$ ceramics in the composite matrix and on the method of sintering. The abrasion resistance of composites is improved with the increasing content of TiB$_2$ in the matrix (Figure 18). In the case of HP-HT sintering, the lowest coefficient of friction was obtained in composites contain-ing 8 vol% of TiB$_2$ (0,54-0,58, depending on the sintering temperature). For comparison, the coefficient of friction of the sintered AISI 316L steel was in the range of 0.67-0.72 (Figure 18a). The addition of TiB$_2$ improves the abrasion resistance of composites. This is the effect of the high hardness of TiB$_2$ ceramics, reaching 3400 HV [56]. TiB$_2$ particles protect the austenitic steel matrix during the process of friction, reducing the rate of wear. Therefore, in composites with lower content of TiB$_2$ (2 vol% and 4 vol%), the Al$_2$O$_3$ ball could penetrate the material of the steel matrix more easily and remove it during operation. Additionally, it was observed that higher sintering temperature reduced the coefficient of friction. The lowest values of the coefficient of friction were obtained for the material sintered at 1300°C. Similar correlations were observed in the specific wear rate of the tested composites (Figure 19a). The specific wear
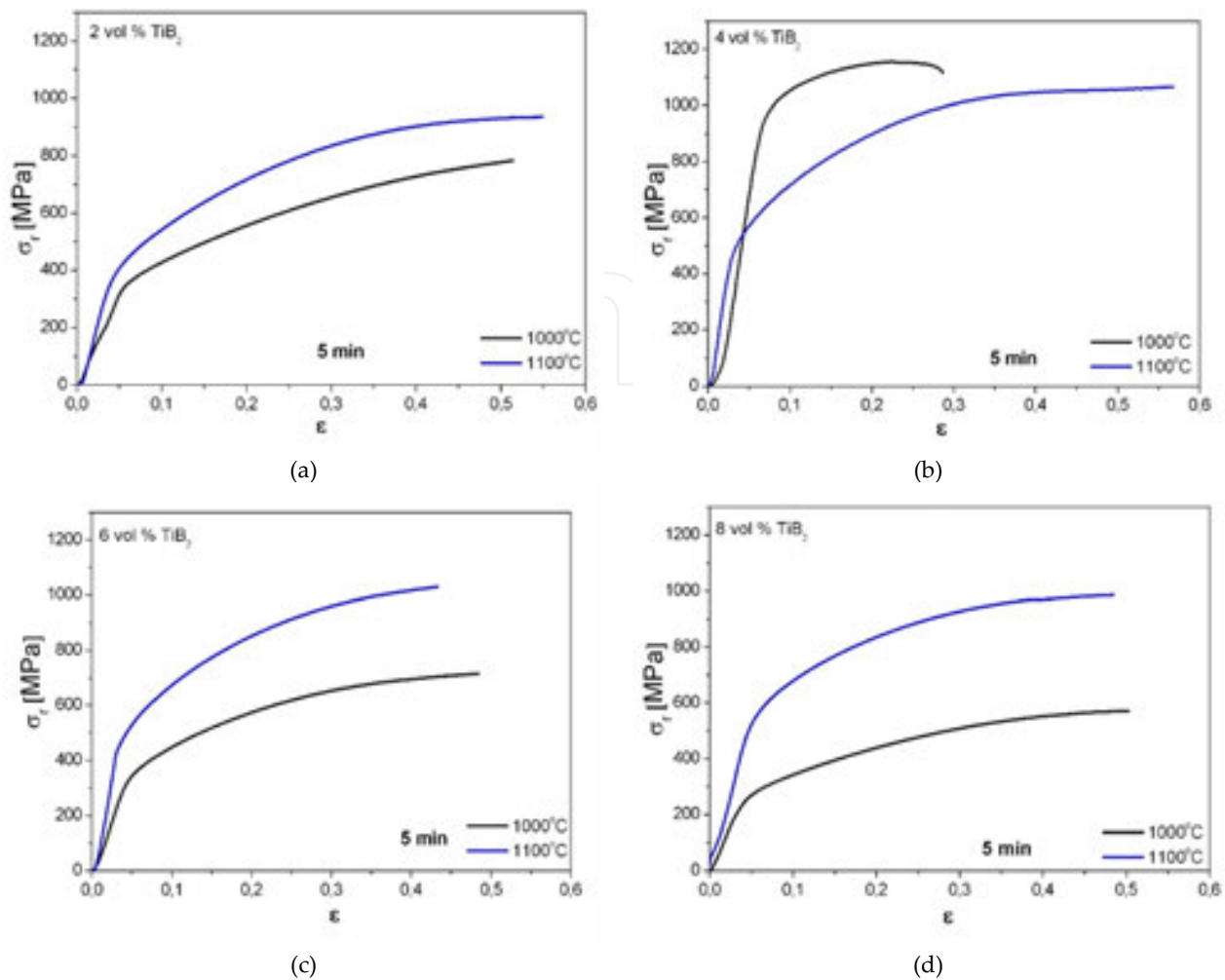
(a)   (b)

(c)   (d)

(e)

Figure 17. Compression strength of the composites with: a) 2 vol% of TiB$_2$ b) 4 vol% of TiB$_2$ c) 6 vol% of TiB$_2$ and d) 8 vol% of TiB$_2$ sintered by SPS method.

rate was decreasing with the increasing content of TiB$_2$ ceramics in the composite matrix. The specific wear rate also depended on the sintering conditions, which means that it was decreasing with the increasing temperature. The lowest value of the specific wear rate was obtained in a composite with 8 vol% of TiB$_2$ ($372*10^{-6}$ mm^3/N • m), while in the AISI 316L steel, it amounted to $599*10^{-6}$ mm^3/N • m (Figure 19a).

Composites sintered by SPS (Figures 18b, 19b) offered improved abrasion resistance, compared with the materials sintered by HP-HT (Figures 18a, 19a). The lowest values of the coefficient of friction and of the specific wear rate were obtained in the materials manufactured by SPS at 1100°C, compared with the materials sintered by HP-HT at a temperature of 1300°C. In the case of these composites (SPS), adding the TiB$_2$ ceramics to the composite matrix considerably reduced the coefficient of friction (Figure 18b). The coefficient of friction assumed the highest value in the austenitic steels (0.62-0.61) and then was gradually decreasing to reach the lowest level in a composite with 8 vol% of TiB$_2$ (0.37). The obtained results prove that tribological properties depend on the parameters of the sintering process. Higher sintering temperature
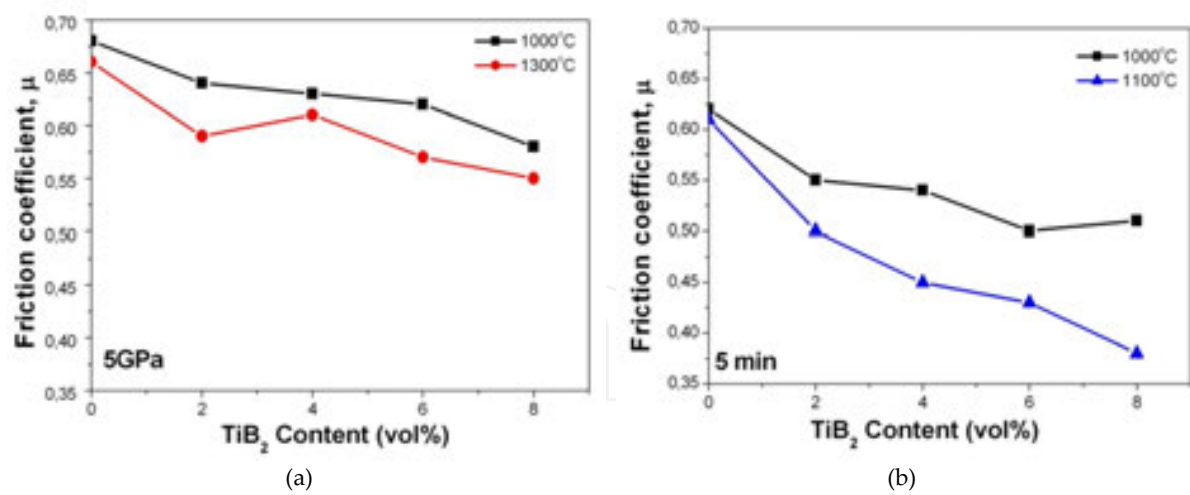
(a)

(b)

Figure 18. Variation of friction coefficient with TiB₂ content for composites sintered by: a) HP-HT [54] and b) SPS [53] method.

reduces the coefficient of friction, and thus the material wear rate. The best tribological properties were obtained in a material sintered at 1100°C for 5 minutes. For these parameters of sintering, the coefficient of friction assumed the values of 0.50, 0.45, 0.43 and 0.37 for composites containing 2 vol%, 4 vol%, 6 vol% and 8 vol% of TiB₂, respectively. By contrast, the specific wear rate was $429*10^{-6}$ [mm³/Nm], $341*10^{-6}$ [mm³/Nm], $314*10^{-6}$ [mm³/Nm] and $299*10^{-6}$ [mm³/Nm] for composites containing 2 vol%, 4 vol%, 6 vol% and 8 vol% of TiB₂, respectively. The results of tribological studies made on the composites fabricated by two different methods of sintering were consistent with the achievements of, among others, Tjong et al. [48,57]. The authors investigated the properties of composites reinforced with different volume fractions of the TiB₂ ceramics (5-20 vol%). Strong beneficial effect of the addition of TiB₂ particles on the abrasion resistance of austenitic stainless steel has been demonstrated.
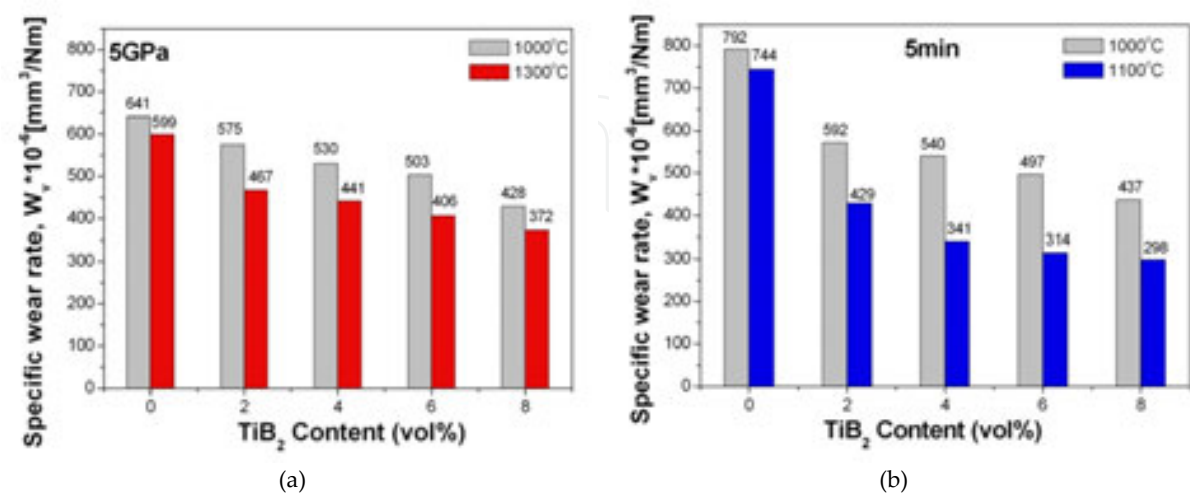

(a)

(b)

Figure 19. Variation of specific wear rate with TiB₂ content for composites obtained by: a) HP-HT [54] and b) SPS [53] method.
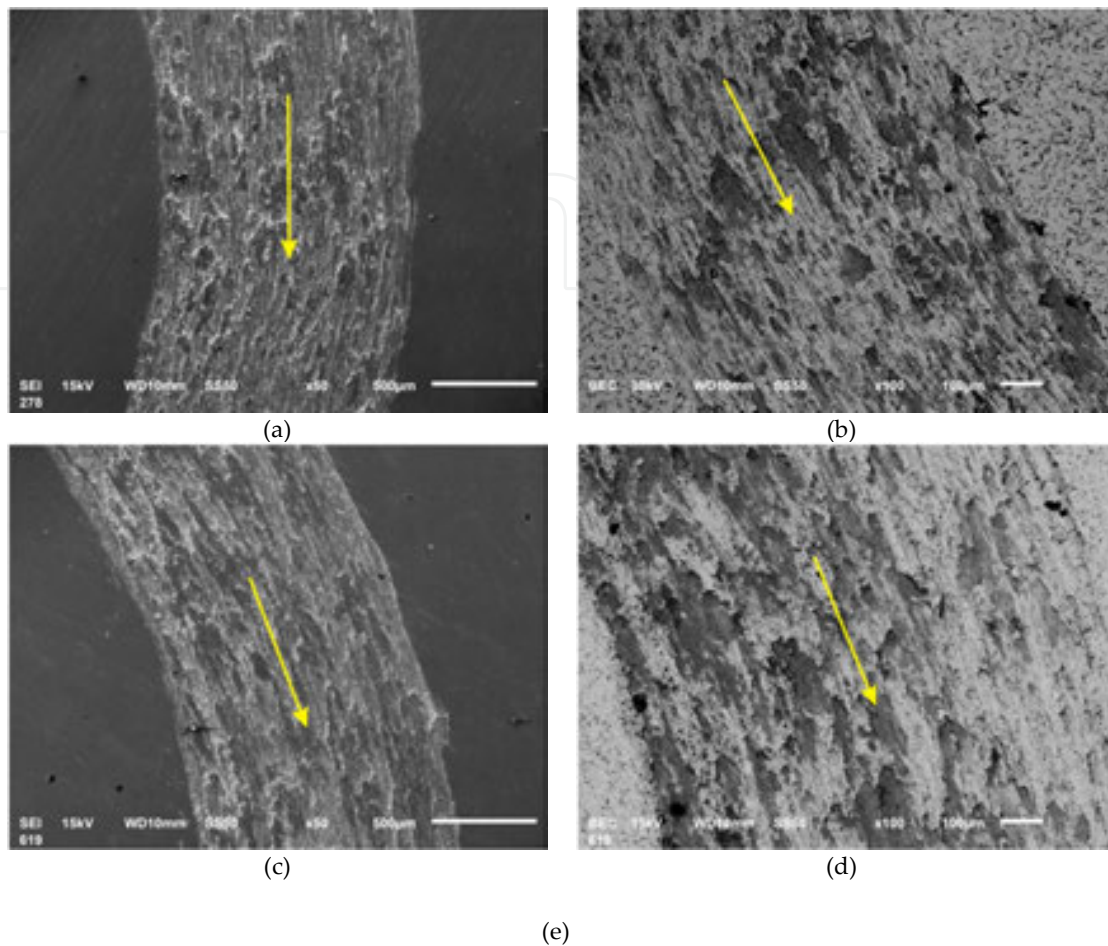
(a)   (b)

(c)   (d)

(e)

Figure 20. Selected SEM micrograph of the worn surface of composites with 8 vol% of TiB_2 obtained by: a, b) HP-HT (sintering temperature of 1300°C) and c, d) SPS (sintering temperature of 1100°C).

Microstructural examinations of wear traces formed in the process of abrasion followed the tribological tests (Figure 20). In all the tested samples, a very similar nature of the material removal by an Al_2O_3 ball was observed. There were visible scratches running parallel to the direction of the ball movement. Comparing wear traces in the composites studied, some characteristic features of the abrasive wear, such as scratches and grooves running in the direction of the ball movement, were observed (light-colour arrows in Figure 20). During abrasion process, permanent deformation of material combined with its attrition has occurred in the place of wear, but no cracks appeared on the worn out surfaces. Microstructural examinations (Figure 20b, d) of the places worn out by abrasion indicated the plastic nature of deformation. In all the tested composites, the surface of the worn out places showed the exposed particles of ceramics and local voids, probably caused by tearing the ceramic phase out of the matrix. The particles of TiB_2 present on the composite surface protected the matrix during abrasion and reduced its wear. This effect was particularly strong in composites reinforced with 6 vol% and 8 vol% of TiB_2.

4. Conclusions

Composite materials based on austenitic stainless steel with varying concentration of TiB_2 ceramics were fabricated. Four variants of the composites were obtained applying the technique of powder metallurgy and the two modern sintering processes, i.e. High Pressure-High Temperature (HP-HT) process and Spark Plasma Sintering (SPS). Based on the results obtained, it has been proved that the introduction of TiB_2 ceramics to the austenitic steel matrix is an efficient way to improve the composite properties. With increasing volume fraction of the reinforcing phase, an improvement in the physical, mechanical and tribological properties was observed. The best composite properties were obtained for the TiB_2 content of 8 vol%.

The study also showed a significant effect of the applied method of sintering on the properties of the tested materials. In all the composites sintered by HP-HT (at 1000°C and 1300°C, 5 GPa) and by SPS (only at 1100°C, 5 min), a very high degree of consolidation was obtained. It was the result of the combined effect of heat and high pressure in the case of the HP-HT method and of the use of electric discharges, high-rate heating and properly selected temperature in the case of the SPS process. Comparing the effect of the sintering methods used it can be concluded that the HP-HT process is a promising method for sintering the TiB_2-reinforced composites. Generally, the materials sintered at temperature of 1300°C and pressure of 5GPa were characterised by optimal microhardness and very good mechanical, plastic and tribological properties. In contrast, the use of SPS reduced the sintering temperature of composites, because already at a temperature of 1100°C and the duration of 5 min sinters with satisfactory density were produced. The best combination of physico-mechanical and tribological properties was obtained in the composites sintered at 1100°C. Careful analysis of the results has showed that the temperature of 1000°C was too low to produce a composite material with high degree of consolidation and satisfactory properties.

The sintering process carried out by either HP-HT or SPS has yielded the composite materials of a uniform and consistent structure produced within the whole volume of the sintered product. A homogeneous distribution of the reinforcing TiB_2 phase was obtained in the matrix of all the sintered products. The reinforcing phase showed a tendency to settle along the matrix grain boundaries. It has been demonstrated that the applied method of sintering and sintering conditions have a significant impact on changes in the microstructure of the tested composites. Application of the SPS process promotes the formation of new phases at the matrix boundary.

Acknowledgements

Author details

Iwona Sulima[*]

Address all correspondence to: isulima@up.krakow.pl

Institute of Technology, Pedagogical University of Cracow, Krakow, Poland

References

[1]   Lis J., Pampuch R., Sintering, Uczelniane Wydawnictwa Naukowo-Dydaktyczne AGH, Kraków, 2000 (in polish).

[2]   Kazior J., Analiza czynników technologicznych decydujących o własnościach spieka‐ nych austenitycznych stali nierdzewnych, Monografia 164, Krakow, Wydawnictwo PK (1994) (in polish)

[3]   Stuijts A. L., Synthesis of Materials from Powders by Sintering, Annual Review of Materials Science 1973; 3, 363-395.

[4]   German R., Sintering: from Empirical Observations to Scientific Principles, Elsevier Inc. March, 2014.

[5]   Kazior J.,' Nykiel M., Pieczonka T., Marcu Puscas T., Molinari A., Activated sintering of P/M duplex stainless steel powders, Journal of Materials Processing Technology, 2004; 157–158, 712–717.

[6]   Bagliuk G, Properties and Structure of Sintered Boron Containing Carbon Steels, Sin‐ tering – Methods and Products, Edited by Dr. Volodymyr Shatokha, Rijeka, Intech; 2012, 249-266 (ISBN 978-953-51-0371-4).

[7]   Celebi Efe G., Yener T., Altinsoy I., Ipek M., Zeytin S., Bindal C., The effect of sinter‐ ing temperature on some properties of Cu–SiC composite, Journal of Alloys and Compounds, 2011; 509 (20), 6036–604.

[8]   Duan X., Jia D., Wu Z., Tian Z., Yang Z., Wang S., Zhou Y., Effect of sintering pres‐ sure on the texture of hot-press sintered hexagonal boron nitride composite ceramics, Scripta Materialia, 2013; 68 (2) 104–107.

[9]   Bundy F.P.; Ultra-high pressure apparatus, Physic Reports, 1988; 3, 156-175.

[10] Jaworska L., Wysokociśnieniowe spiekanie proszków diamentowych, Prace IOS, se‐ ria Zeszyty Naukowe Kraków, 82, 2002 (in polish).

[11] Eremts M.I., High pressure experimental method, Oxford University Press, 1996.

[12] Klimczyk P., Figiel P., Petrusha I., Olszyna A., Cubic boron nitride based composites for cutting applications, Journal of Achievements in Materials and Manufacturing Engineering 2011; 44 (2) 198-204.

[13] Sulima I., Figiel P., Suśniak M., Świątek M., Sintering of TiB$_2$ ceramic, Archives of Materials Science and Engineering, 2007; 28 (11) 687-690.

[14] Rozmus M. „Cermetalowe materiały gradientowe", Materiały Ceramiczne, 2006; 4,142-147 (in polish).

[15] Rozmus M., Jaworska L., Królicka B., Putyra P., Gradientowa mikrostruktura kompozytowych spieków diamentowych przeznaczonych na narzędzia skrawające, Materiały Ceramiczne /Ceramic Materials, 2009; 61 (3) 192-196 (in polish).

[16] Wyżga P., Jaworska L., Bućko M., Putyra P., Kalinka A., Sintering of TiB$_2$-TiN nano- and micropowders, Composite Theory and Practice, 2011; 1, 34-38.

[17] Sulima I., Klimczyk P., Hyjek P., The influence of the temperature and pressure on the properties of the AISI 304L stainless steel reinforced with TiB$_2$ ceramic, Archives of Materials Science and Engineering, 2009; 39 (2)103-106.

[18] Sulima I., Jaworska L., Wyżga P., Perek-Nowak M.,The influence of reinforcing particles on mechanical and tribological properties and microstructure of the steel-TiB$_2$ composites, Journal of Achievements in Materials and Manufacturing Engineering, 2011; 48 (1) 52-57.

[19] Figiel P., Jaworska L., Putyra P., Klimczyk P., Bryła K., Wysokociśnieniowe i swobodne spiekania kompozytów cermetalowych z udziałem nanometrycznych proszków TiC, Composite Theory and Practice, 2008, 130-135 (in polish).

[20] Taylor G.F.: Apparatus for Making Hards Metal Compositions, U.S. Patent No. 1896854, 1933

[21] Orru R., Licheri R., Cincotti A. M., Cao G.: Consolidation/synthesis of materials by electric current activated/assisted sintering, Materials Science and Engineering 2009; 63, 127-134.

[22] Inoue K., US Patent No. 3 24,1956

[23] Omori M., Sakai H., Okubo A., Kawahara M., Tokita M., Hirai T., Preparation and Properties of ZrO$_2$(3Y)/Ni FGM, Proceedings of the 3rd International Symposium on Structural and Functionally Gradient Materials, Lausanne, Switzerland, 1994; 99-104.

[24] Omori M., Sakai H., Okubo A., Tokita M., Kawahara M., T. Hirai, Preparation of Functional Gradient Materials by Spark Plasma Sintering, Symposium of Materials Research Society of Japan, 1994.

[25] Yoshimura M., Ohji T., Sando M. Nihara K., Rapid rate sintering of nano-grained ZrO$_2$-based composites using pulse electric current sintering method. Journal of Materials Science Letters, 1998; 17, 1389-1391.

[26] Tokita M.: Mechanism of Spark Plasma Sintering. 1996 http://xa.yimg.com/kq/groups/3862917/2054596553/name/SUMITOMO+REVIEW-Spark-Plasma-Sintering.pdf.

[27] Omori M., Sintering, consolidation, reaction and crystal growth by the spark plasma system (SPS), Materials Science Engineering, 2000; A287; 183-188.

[28] Peng H., Spark Plasma Sintering of Si_3N_4-Based Ceramics-Sintering mechanism-Tailoring microstructure-Evaluating properties, PhD thesis, Department of Inorganic Chemistry, Stockholm University, 2004.

[29] Tokita M., Trends in Advanced SPS Spark Plasma Sintering Systems and Technology, Journal of the Society of Powder Technology Japan, 1993; 30 (11) 790-804.

[30] Tokita M., Mechanism of spark plasma sintering, Proceeding of NEDO International Symposium on Functionally Graded Materials, Kyoto, Japan, 1999, 23-33.

[31] Zang J., Field Activated Sintering Technology: Multi-physics Phenomena Modelling, A Coupled Thermal-electrical-densification Framework, Lambert Academic Publishing, Saarbrücken, 2010.

[32] Putyra, P., Figiel P., Podsiadło M., Klimczyk P., Alumina composites with solid lubricant participations, sintered by SPS-method, Kompozyty, 2011; 2, 107-110.

[33] Pellizzari M., Fedrizzi A., Zadra M., Influence of processing parameters and particle size on the properties of hot work and high speed tool steels by Spark Plasma Sintering, Materials and Design, 2011; 32, 1796–1805.

[34] Venkateswaran T., Basu B., Raju G.B., Kim D.Y., Densification and properties of transition metal borides-based cermets via spark plasma sintering, Journal of the European Ceramic Society 2006; 26, 2431–2440.

[35] Dustin D. M., Dongtao J., Dina V. D., Mukherjee A. K., The synthesis and consolidation of hard materials by spark plasma sintering, International. Journal of Refractory Metals & Hard Materials, 2009; 27, 367–375.

[36] Material Science and Engineering Handbook, Ed. James F. Shackelford, Second Edition by CRC Press, Florida, 2001.

[37] Raju G.B, Mukhopadhyay A., Biswas K., Basu B., Densification and high-temperature mechanical properties of hot pressed TiB_2–(0–10 wt.%) $MoSi_2$ composites, Scripta Mater. 2009; 61, 674-6.

[38] Konigshofer R., Furnsinn S., Steinkellner P., Lengauer W., Haas R., Rabitsch K., Scheerer M., Solid-state properties of hot-pressed TiB_2 ceramics, International Journal of Refractory Metal and Hard Materials, 2005; 23 350–357.

[39] Wang F. C., Zhang Z. H., Luo J., Huang C. C., Lee S. K., A novel rapid route for in situ synthesizing TiB-TiB_2 composites, Composites Science and Technology, 2009; 69 (15-16) 2682–2687.

[40] Matkovich, V. I., Boron and Refractory Borides. Springer, Berlin, 1977; 172.

[41] Balcı Ö., Ağaoğulları D., Gökçe H., Duman İ., Öveçoğlu M. L, Influence of TiB$_2$ particle size on the microstructure and properties of Al matrix composites prepared via mechanical alloying and pressureless sintering, Journal of Alloys and Compounds, 2014; 586 (1) S78–S84.

[42] Kwon Y.-S., Kim H.-T., Kim j.-S., Dudina D.V., Spark plasma sintering of Cu-TiB$_2$ nanocomposite, Novel Materials Processing by Advanced Electromagnetic Energy Sources, Proceedings of the International Symposium on Novel Materials Processing by Advanced Electromagnetic Energy Sources March 19–22, Osaka, Japan, 2005; 293–296.

[43] Jaroszewicz J., Michalski A., Preparation of a TiB$_2$ composite with a nickel matrix by pulse plasma sintering with combustion synthesis, Journal of the European Ceramic Society, 2006; 26 (13) 2427–2430.

[44] Animesh A., Bandyopadhyay T.K., Das K., Synthesis and characterization of TiB$_2$-reinforced iron-based composites, Journal of Materials Processing Technology, 2006; 172, 70–76.

[45] Tjong S.C., Tam K., F., Mechanical and thermal expansion behaviour of hipped aluminium-TiB$_2$ composites", Materials Chemistry and Physics, 2006; 97, 91-97.

[46] Pettersson A., Magnusson P., Lundberg P., Nygren M., Titanium–titanium diboride composites as part of a gradient amour material, International Journal of Impact Engineering, 2005; 32, 387–399.

[47] Nahme H., Lach E., Tarran A., Mechanical property under high dynamic loading and microstructure evaluation of a TiB2 particle-reinforced stainless steel, Journal of Materials Science, 2009; 44, 463-468.

[48] Tjong S.C., Lau K.C. Abrasion resistance of stainless-steel composites reinforced with hard TiB$_2$ particles, Composites Science and Technology, 2000; 60 (8) 1141-1146.

[49] International Standard, Fine ceramics (advanced ceramics, advanced technical ceramics)-Determination of friction and wear characteristics of monolithic ceramics by ball-on-disc method, ISO 20808:2004(E).

[50] Meozzi M., Special use of the ball on disc standard test, Tribology International, 2006; 39 (6) 496–505.

[51] Sulima I., Figiel P., Kurtyka P., Austenitic stainless steel –TiB$_2$ composites obtained by HP-HT method, Composites Theory and Practice, 2012; 12 (4) 245-250.

[52] Sulima I., L.Jaworska, P.Figiel, Influence of processing parameters and different content of TiB$_2$ ceramics on the properties of composites sintered by high temperature – high pressure (HT-HP) method, Archives of Metallurgy and Materials, 2014; 59 (1) 203-207.

[53] Sulima I. Tribological properties of steel/TiB$_2$ composites prepared by spark plasma sintering, Archives of Metallurgy and Materials (2014; in press).

[54] Sulima I, P. Klimczyk, P.Malczewski, Effect of TiB$_2$ particles on the tribological properties of stainless steel matrix composites, Acta Metallurgica Sinica (English Letter), 2014; 27(1), 12–18.

[55] CRC Materials Science and Engineering Handbook, Third Edition Edited by James F. Shackelford and William Alexander CRC Press, 2001, 509.

[56] McGuire M. F., Stainless Steels for Design Engineers, ASM International, 2008, 69-78.

[57] Tjong K.C., Lau K.C., Sliding wear of stainless steel matrix composite reinforced with TiB$_2$ particles, Materials Letters, 1999; 4 (4) 153-158.